

## Antiproliferative Effects of CDK4/6 Inhibition in CDK4-Amplified Human Liposarcoma *In Vitro* and *In Vivo*

Yi-Xiang Zhang<sup>1,2</sup>, Ewa Sicinska<sup>1,3</sup>, Jeffrey T. Czaplinski<sup>1,3</sup>, Stephen P. Remillard<sup>1,2</sup>, Samuel Moss<sup>1,3</sup>, Yuchuan Wang<sup>4</sup>, Christopher Brain<sup>5</sup>, Alice Loo<sup>5</sup>, Eric L. Snyder<sup>6,7</sup>, George D. Demetri<sup>1,2</sup>, Sunkyu Kim<sup>5</sup>, Andrew L. Kung<sup>8</sup>, and Andrew J. Wagner<sup>1,2</sup>

### Abstract

Well-differentiated/dedifferentiated liposarcomas (WD/DDLPS) are among the most common subtypes of soft tissue sarcomas. Conventional systemic chemotherapy has limited efficacy and novel therapeutic strategies are needed to achieve better outcomes for patients. The cyclin-dependent kinase 4 (*CDK4*) gene is highly amplified in more than 95% of WD/DDLPS. In this study, we explored the role of CDK4 and the effects of NVP-LEE011 (LEE011), a novel selective inhibitor of CDK4/CDK6, on a panel of human liposarcoma cell lines and primary tumor xenografts. We found that both CDK4 knockdown by siRNA and inhibition by LEE011 diminished retinoblastoma (RB) phosphorylation and dramatically decreased liposarcoma cell growth. Cell-cycle analysis demonstrated arrest at G<sub>0</sub>-G<sub>1</sub>. siRNA-mediated knockdown of RB rescued the inhibitory effects of LEE011, demonstrating that LEE011 decreased proliferation through RB. Oral administration of LEE011 to mice bearing human liposarcoma xenografts resulted in approximately 50% reduction in tumor <sup>18</sup>F-fluorodeoxyglucose uptake with decreased tumor biomarkers, including RB phosphorylation and bromodeoxyuridine incorporation *in vivo*. Continued treatment inhibited tumor growth or induced regression without detrimental effects on mouse weight. After prolonged continuous dosing, reestablishment of RB phosphorylation and cell-cycle progression was noted. These findings validate the critical role of CDK4 in maintaining liposarcoma proliferation through its ability to inactivate RB function, and suggest its potential function in the regulation of survival and metabolism of liposarcoma, supporting the rationale for clinical development of LEE011 for the treatment of WD/DDLPS. *Mol Cancer Ther*; 13(9); 2184–93. ©2014 AACR.

### Introduction

The retinoblastoma (RB) tumor-suppressor protein plays a critical role in regulating cellular proliferation, and loss of function of the RB protein is commonly found in human malignancies (1, 2). RB function is

regulated by phosphorylation of multiple serine and threonine residues, initiated during the G<sub>1</sub>-S cell-cycle transition by cyclin-dependent kinases (CDK) 4 or 6 (3–5). These enzymes, in turn, are activated by temporal expression of cyclin D, and inhibited by the CDK inhibitor p16 (6, 7). Multiple mechanisms for dysregulation of this pathway in cancer have been identified, including mutation or loss of expression of RB (2), overexpression of cyclin D (8, 9), loss of p16 (10), and mutation, genomic amplification, or overexpression of CDK4 (11).

More than 95% of human well-differentiated/dedifferentiated liposarcomas (WD/DDLPS) exhibit dysregulation of CDK4 through high-level amplification of a region of the long arm of chromosome 12 containing this gene (12, 13). WD/DDLPS represent one of the most common forms of soft tissue sarcomas (14, 15). WDLPS is a typically indolent, non-metastasizing disease that can be cured by surgical excision, although local recurrences are common. DDLPS may arise from WDLPS or *de novo*, and may also be cured by surgical resection, although its rapid growth rate, predilection for retroperitoneal growth, and ability to be locally destructive or metastasize frequently result in recurrences and patient mortality. Clinical benefit from conventional systemic chemotherapy is limited, transient, and often toxic, indicating that newer therapeutic strategies are needed to better treat this disease (16, 17).

<sup>1</sup>Ludwig Center at Dana-Farber/Harvard, Harvard Medical School, Boston, Massachusetts. <sup>2</sup>Department of Medical Oncology, Center for Sarcoma and Bone Oncology, Dana-Farber Cancer Institute, Boston, Massachusetts. <sup>3</sup>Department of Medical Oncology, Center for Molecular Oncologic Pathology, Dana-Farber Cancer Institute, Boston, Massachusetts. <sup>4</sup>Department of Radiology, Johns Hopkins School of Medicine, Baltimore, Maryland. <sup>5</sup>Novartis Institutes for Biomedical Research, Cambridge, Massachusetts. <sup>6</sup>Department of Pathology, Brigham and Women's Hospital, Harvard Medical School, Boston, Massachusetts. <sup>7</sup>Koch Institute for Integrative Cancer Research, Massachusetts Institute of Technology, Cambridge, Massachusetts. <sup>8</sup>Department of Pediatrics, Columbia University Medical Center, New York, New York.

**Note:** Supplementary data for this article are available at Molecular Cancer Therapeutics Online (<http://mct.aacrjournals.org/>).

Current address for Eric L. Snyder: Departments of Pathology and Anatomy, School of Medicine, University of California, San Francisco, San Francisco, CA.

**Corresponding Author:** Andrew J. Wagner, Center for Sarcoma and Bone Oncology, Dana-Farber Cancer Institute, 450 Brookline Avenue, Boston, MA 02215. Phone: 617-632-5204; Fax: 617-632-3408; E-mail: Andrew\_Wagner@dfci.harvard.edu

doi: 10.1158/1535-7163.MCT-14-0387

©2014 American Association for Cancer Research.

One potential approach to treatment of liposarcoma is through targeting the enzymatic activity of CDK4 with novel small-molecule inhibitors. Previous studies have preliminarily demonstrated the *in vitro* effects of CDK4 inhibition in liposarcoma cells: Helias-Rodzewicz and colleagues first reported that treatment of a liposarcoma cell line with the CDK4 inhibitor NSC625987 decreased cell proliferation and induced adipocytic differentiation (18). Barretina and colleagues showed cell-cycle arrest and growth inhibition in two liposarcoma cell lines treated with CDK4 shRNA or the CDK4/6 inhibitor PD0332991 (19). A more recent study also reported that the addition of an IGF1R inhibitor to PD0332991 led to greater inhibition of cell-cycle progression and cell metabolic activity (20). However, detailed biochemical analyses and the preclinical *in vivo* effects of CDK4/6 inhibitors on liposarcoma xenograft models have not yet been described, and predictive biomarkers for CDK4/6 inhibitor activity are still lacking. Recently, several CDK4/6 inhibitors have entered into clinical development, and an exploratory clinical trial suggested activity against liposarcoma (21). In this study, we explore the biochemical, antiproliferative, and antimetabolic effects of CDK4 inhibition in more detail than has previously been reported, using siRNA and the novel small-molecule CDK4/6 inhibitor NVP-LEE011 (LEE011) in both cell line and patient-derived tumor xenograft models of WD/DDLPS.

## Materials and Methods

### Cell lines and cell culture

Human WD/DDLPS cell lines 449 and 778 (also called 93449 or T449 and 94778 or T778; ref. 22) were kindly provided by Dr. Florence Pedeutour (Université de Nice-Sophia Antipolis, Nice, France) and Dr. David Thomas (Peter MacCallum Cancer Centre, Melbourne, Australia) in 2008; LPS141 (23) was kindly provided by Dr. Jonathan A. Fletcher (Brigham and Women's Hospital, Boston, MA) in 2008; LP3, LP6 (23), and LP8 were generated at Dana-Farber Cancer Institute (Boston, MA) in 2008. Cell lines were cultured in RPMI-1640 supplemented with 15% FBS (Hyclone), 1× penicillin-streptomycin-amphotericin B (Invitrogen), and 1× glutamax (Invitrogen) at 37°C in a humidified incubator with 95% air and 5% CO<sub>2</sub>. Human white preadipocyte primary cells were purchased from PromoCell (C-12732, Lot# 0071202.27) and cultured in the Preadipocyte Growth Medium (PromoCell). For differentiation of human preadipocytes, confluent preadipocyte cultures were incubated with Preadipocyte Differentiation Medium (PromoCell) for 72 hours, and then changed to Adipocyte Nutrition Medium (PromoCell) for 14 days. Adipogenic differentiation was confirmed via Oil red O staining as previously described (24). Liposarcoma cell lines were characterized by high-resolution short tandem repeat profiling with Promega PowerPlex 1.2 system at the Molecular Diagnostics Laboratory of Dana-Farber Cancer Institute. The cells used for the experiment are passaged for less than 6 months after authentication.

### Inhibitors and siRNA

The CDK4/6 inhibitor NVP-LEE011 (succinate salt, powder form; LEE011) was synthesized by the Novartis Institutes for Biomedical Research (Cambridge, MA; ref. 25). ON-TARGETplus siRNA against *RB1* (#J-003296–10, 13), *CDK4* (#J-003238–12, 13), and scrambled control were purchased from Dharmacon. Cells were transfected with siRNA at a final concentration of 3.12 to 6.25 nmol/L with RNAiMAX (Invitrogen) according to the manufacturer's protocol.

### Copy-number analysis

Gene copy number was determined by probe-based qRT-PCR using StepOnePlus real-time PCR system (Applied Biosystems). Human male normal genomic DNA was purchased from PE Biosystems. Genomic DNA from cell cultures was extracted using the DNeasy blood and tissue kit (Qiagen). Primers and probes were obtained from the TaqMan copy-number assays catalog of Applied Biosystems (CDK4, Hs06345580\_cn; RNase P, 4403326). The *Rnase P* gene was used as an internal normalization reference. Each reaction was performed in a total volume of 20 μL, containing 1× TaqMan Genotyping Master Mix, 1× CDK4 Primer-Probe Mix, 1× RNase P Primer-Probe Mix, and 20 ng genomic DNA. All reactions were performed in quadruplicate and repeated at least three times. PCR thermocycling conditions consisted of an initial step at 95°C for 10 minutes, followed by 40 cycles of 15 seconds at 95°C and 1 minute at 60°C. The threshold cycle (C<sub>t</sub>) level for tested genes was automatically determined by the StepOnePlus Software. *CDK4* copy number was determined by Copy-Caller software (version 1.0; Applied Biosystems) using human normal genomic DNA as a calibrator sample.

### Immunoblot analyses

Cells were lysed on ice in lysis buffer containing 50 mmol/L HEPES (pH 7.5), 150 mmol/L NaCl, 1 mmol/L EGTA, 10% Glycerol, 1% Triton X-100, 100 mmol/L NaF, 10 mmol/L Na<sub>4</sub>P<sub>2</sub>O<sub>7</sub>·10 H<sub>2</sub>O, 1 mmol/L Na<sub>3</sub>VO<sub>4</sub>, and 1× Complete Protease Inhibitor Cocktail (Roche Diagnostics). Antibodies for immunoblotting were purchased from Santa Cruz Biotechnology (CDK4 #sc-260); Sigma (α-tubulin #T9026); and Cell Signaling Technology [p-RB (Ser780) #9307, p-RB (Ser807/811) #9308, RB #9309, CDK6 #3136, Cyclin D1 #2978, Cyclin D2 #3741, Cyclin D3 #2936, p15 #4822, p16 #4824, p18 #2896]. Chemiluminescent signal was captured with X-ray film.

### Cell proliferation assay

Cells were exposed to various treatments (inhibitor, siRNA, or vehicle control) for times as indicated. Cell numbers were determined using a Neubauer hemocytometer.

To determine the half maximal growth inhibitory concentration (GI<sub>50</sub>) values of LEE011 in liposarcoma cells, cell numbers were counted before treatment (T<sub>0</sub>) and after 3 days of vehicle control (C) or LEE011 treatment (T). Drug response was calculated following the formula: The percentage of growth = 100 × (T – T<sub>0</sub>)/(C – T<sub>0</sub>). GI<sub>50s</sub>

were determined using sigmoidal dose–response (variable slope) curve fitting with Prism 5 software (GraphPad Software).

#### Cell-cycle analysis by flow cytometry

Cells were exposed to inhibitors or 0.1% DMSO for 24 hours and harvested. After washing with ice-cold PBS, cells were fixed in 70% ethanol at 4°C for at least 2 hours. Fixed cells were stained in PBS containing 10 µg/mL RNase A and 20 µg/mL propidium iodide (Sigma) in the dark. DNA content analysis was performed by flow cytometry (FACSCalibur; BD Biosciences) with CellQuest and ModFIT LT software (BD Biosciences).

#### Establishment of cell line and patient-derived human liposarcoma xenograft models

The LPS3 primary human liposarcoma xenograft model was established by implanting fresh human liposarcoma tissue fragments into the subcutaneous tissue of female nude mice (Nu/Nu; Charles River Laboratories) after signed informed consent was previously obtained from a patient undergoing surgery, according to an Institutional Review Board–approved research protocol. LPS3 tumor xenografts were serially passaged as subcutaneous implants of tumor fragments approximately 2 mm in diameter derived from tumors less than 1,000 mm<sup>3</sup>.

The LP6 cell line was derived from the same patient's liposarcoma tissue, and for cell line xenograft experiments approximately  $1 \times 10^6$  cells were suspended in PBS, mixed 1:1 with Matrigel (BD Biosciences), and subcutaneously injected into female nude mice (Nu/Nu; Charles River Laboratories) in a final volume of 100 µL.

The HSAX2655 tumor was obtained under collaboration with the National Cancer Institute (Bethesda, MD), and originated from a retroperitoneal liposarcoma. Tumor xenografts were serially passaged in female nude mice (Harlan Laboratories) as subcutaneous implants of tumor fragments approximately 3 mm in diameter.

#### In vivo bromodeoxyuridine incorporation assay

Mice bearing LP6 tumors (>200 mm<sup>3</sup>) were treated with 250 mg/kg LEE011 formulated as a 25 mg/mL suspension in 0.5% methylcellulose (#S80080; Fisher Scientific) or vehicle control by oral gavage for three daily doses. Bromodeoxyuridine (BrdUrd) solution (10 mg/mL, 0.2 mL/mouse) was injected i.p. 16 hours after the last dose of study drug or control. After 2 additional hours, mice were sacrificed and tumors were fixed in 10% formalin for immunohistochemistry (IHC) analysis or snap frozen for immunoblot analysis.

#### <sup>18</sup>F-FDG-PET functional imaging study

Matched cohorts of mice with LP6 tumors (300 mm<sup>3</sup> average) were randomly assigned to treatment with LEE011 (250 mg/kg) or vehicle control by oral gavage for three daily doses. Before randomization (T<sub>0</sub>) and after 3 days of therapy (T<sub>3</sub>), mice were evaluated by 2-[<sup>18</sup>F]-fluoro-2-deoxy-D-glucose (FDG)-PET imaging (26). Each

mouse was fasted overnight before imaging and then was administered approximately 400 µCi <sup>18</sup>F-FDG (~0.2 mL) through intraperitoneal injection. Mice were warmed and awake during a 60-minute tracer uptake period, and then anesthetized before undergoing 10-minute PET scan. The maximum standardized uptake value (SUV<sub>max</sub>) in tumor was recorded, and the change in SUV<sub>max</sub> after therapy was calculated as the percentage of change  $SUV_{max} = 100 \times (SUV_{max}(T_3) - SUV_{max}(T_0)) / SUV_{max}(T_3)$ .

#### In vivo efficacy studies

Mice bearing LPS3 tumor xenografts (>2 mm in diameter and with volumes <100 mm<sup>3</sup>) were randomized into statistically identical cohorts (6 mice/group), and treated with 250 mg/kg LEE011 or with vehicle alone by oral gavage following a 5 days on and 2 days off schedule for 3 weeks. Mice with established LP6 cell line xenograft tumors (average tumor volume >250 mm<sup>3</sup>) were randomized into statistically identical cohorts (≥8 mice/group), and treated with 250 mg/kg LEE011 or with vehicle alone by oral gavage daily for 21 days. Tumor size was measured by caliper every 3 to 6 days, and volume was calculated using the formula: Volume = 0.5 × L × W<sup>2</sup>. Mouse body weight was recorded every 3 to 7 days. Mice were sacrificed when the tumor diameter reached 2 cm.

Mice bearing HSAX2655 tumor xenografts were treated with 250 mg/kg LEE011 or vehicle control daily by oral gavage beginning 35 days postimplantation (4 mice in control group, 12 mice in LEE011 group), when the tumor volume reached an average size of 258 mm<sup>3</sup>, and continued for 80 days at which point drug treatment was suspended. Mice with tumors that regrew were retreated with 250 mg/kg LEE011 daily when tumors reached a volume of >500 mm<sup>3</sup>. Body weight and tumor volume were recorded twice weekly.

All procedures were performed according to protocols approved by the Institutional Animal Care and Use Committees of the Dana-Farber Cancer Institute or Novartis Biomedical Research Institutes.

#### IHC

IHC was performed on 4-µm sections of formalin-fixed paraffin-embedded samples. Tissue sections were deparaffinized and rehydrated, and antigen retrieval was performed in 10 mmol/L citrate buffer (pH 6.0) in a 750 W microwave oven at 199°C for 30 minutes for BrdUrd staining, and in a pressure cooker at 120°C for 5 minutes followed by 90°C for 10 seconds for phospho-RB staining. Phospho-RB (Ser780; Abcam, Ab47763), or BrdUrd primary antibody (BD Biosciences, #347580) was added at a dilution of 1:100 and incubated for 1 hour at room temperature. Sections were further processed with horseradish peroxidase-conjugated secondary antibody. The reaction was detected by 3,3-diaminobenzidine and hematoxylin staining. Images were obtained with an Olympus CX41 microscope and QCapture software (QImaging).

### Statistical analysis

Comparisons between groups were made using the two-tailed unpaired *t* test. Differences in mean  $\pm$  SEM with  $P < 0.05$  were considered statistically significant.

### Results

#### RB is highly expressed and strongly phosphorylated in human liposarcoma cells

We determined *CDK4* copy number in the six liposarcoma cell lines and the LPS3 and HSAX2655 primary human liposarcoma xenografts and found high-level *CDK4* gene amplification (Fig. 1A and data not shown) in each, recapitulating the setting of liposarcoma tumors. Correspondingly, CDK4 protein was expressed at a higher level in liposarcoma cells in comparison with normal preadipocytes and adipocytes (Fig. 1B).

We then examined the expression and phosphorylation level of RB as well as the status of other G<sub>1</sub>-S transition regulatory proteins in liposarcoma cells. As shown in Fig. 1B, RB was highly expressed and strongly phosphorylated at the CDK4/6-specific sites Ser780 and Ser807/811 (5) in liposarcoma cells in comparison with normal preadipocytes and adipocytes. Cyclin D1, p15, and p16 were expressed in all of the liposarcoma cell lines. CDK6 and cyclin D2 were only detectable in a subset. These data demonstrate increased CDK4 and RB expression/activity in human liposarcoma cells.

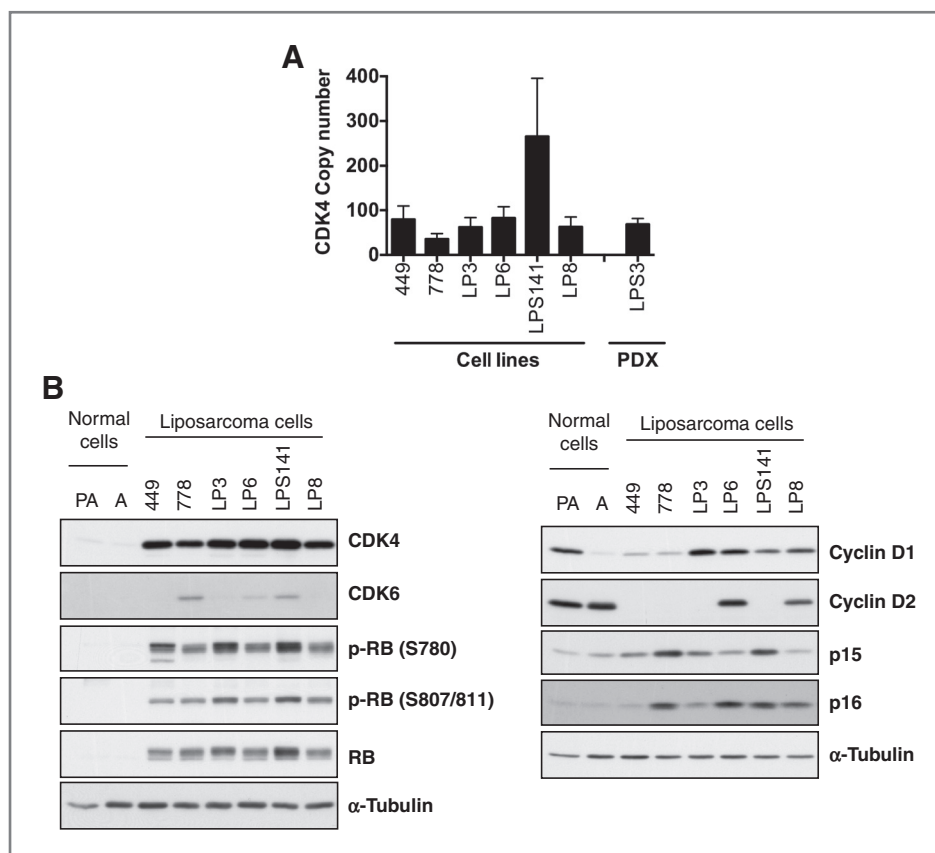
#### CDK4 knockdown inhibits RB phosphorylation and cell growth in liposarcoma cells

To explore the role of CDK4 in regulation of RB phosphorylation and cell growth, we applied CDK4 siRNAs to LP6 liposarcoma cells and investigated their biologic effects. As shown in Fig. 2A, the expression of CDK4 was dramatically decreased by CDK4 siRNAs. CDK4 knock-down resulted in a decrease in RB phosphorylation at the CDK4-specific sites Ser807/811 compared with controls (Fig. 2A). Moreover, growth in CDK4 siRNA-transfected cells was completely blocked at 24 hours after transfection (Fig. 2B). These results demonstrate that CDK4 is a major regulator of RB phosphorylation and cell growth in liposarcoma cells.

#### LEE011, a selective CDK4/6 inhibitor, inhibits RB phosphorylation, and blocks cell proliferation in liposarcoma cells

LEE011 is a novel, selective CDK4/6 inhibitor in clinical development (Supplementary Fig. S1; refs. 25, 27). To demonstrate its impact on tumor cells *in vitro*, we examined the effects of LEE011 in liposarcoma cells. LEE011 reduced RB phosphorylation at Ser780 and Ser807/811 in both a concentration- and time-dependent manner with complete inhibition at 3.33  $\mu$ mol/L (Fig. 3A and B; Supplementary Fig. S2). Correspondingly, 0.04 to 3.33  $\mu$ mol/L LEE011 decreased LP6 cell growth in a concentration-dependent

**Figure 1.** *CDK4* copy number and expression of cell-cycle regulatory proteins in liposarcoma cells. **A**, *CDK4* copy number in liposarcoma cells and a patient-derived xenograft (PDX) was determined by qRT-PCR with the *Rnase P* gene as an internal normalization reference and human normal genomic DNA as a calibrator sample. Values represent mean  $\pm$  SD ( $n \geq 3$ ). **B**, protein expression was analyzed by immunoblot analyses. PA, preadipocytes; A, adipocytes.



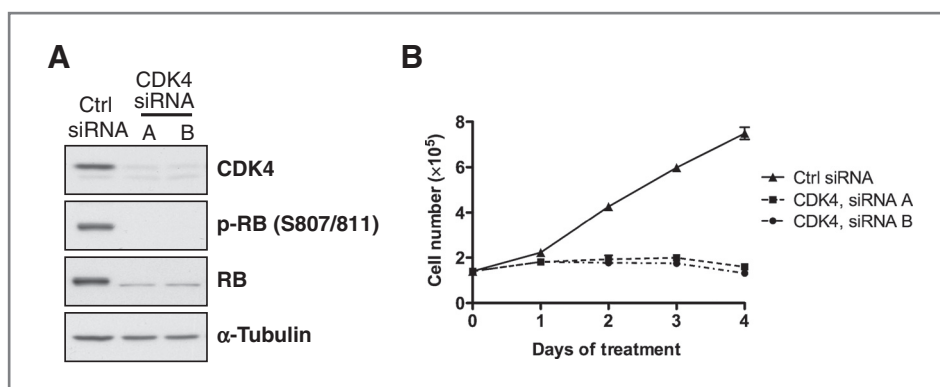


**Figure 2.** Effects of siRNA-mediated knockdown of CDK4 on RB phosphorylation and cell growth in liposarcoma cells. **A**, effects of CDK4 knockdown on RB phosphorylation were examined by immunoblot analysis at 40 hours in LP6 liposarcoma cells. **B**, effects of CDK4 knockdown on growth of LP6 cells were monitored daily by cell counting.

manner, with sustained growth arrest following 24 hours of treatment of 1.11 and 3.33  $\mu\text{mol/L}$  LEE011 (Fig. 3C and D). Cell-cycle analysis demonstrated cell-cycle arrest at  $G_0$ - $G_1$  and a decreased proportion of cells in S phase following 24 hours of exposure to LEE011 (Fig. 3E).

The growth inhibitory potential of LEE011 was examined in five additional liposarcoma cell lines, and similar effects were observed in each (Fig. 3D and 3F). LEE011 inhibited cell growth in a concentration-dependent manner with  $GI_{50}$  value of 0.13 to 0.24  $\mu\text{mol/L}$  (Fig. 3D) and

complete inhibition at 3.33  $\mu\text{mol/L}$ , and dramatically decreased the proportion of cells in S phase (Fig. 3F). These data demonstrate the ability for LEE011 to induce cell-cycle arrest and inhibit cell growth in a variety of liposarcoma cell lines.

#### LEE011 inhibited liposarcoma cell-cycle progression in a RB-dependent manner

To determine the specificity of the inhibitory effects of LEE011 on cell-cycle progression, we transfected cells

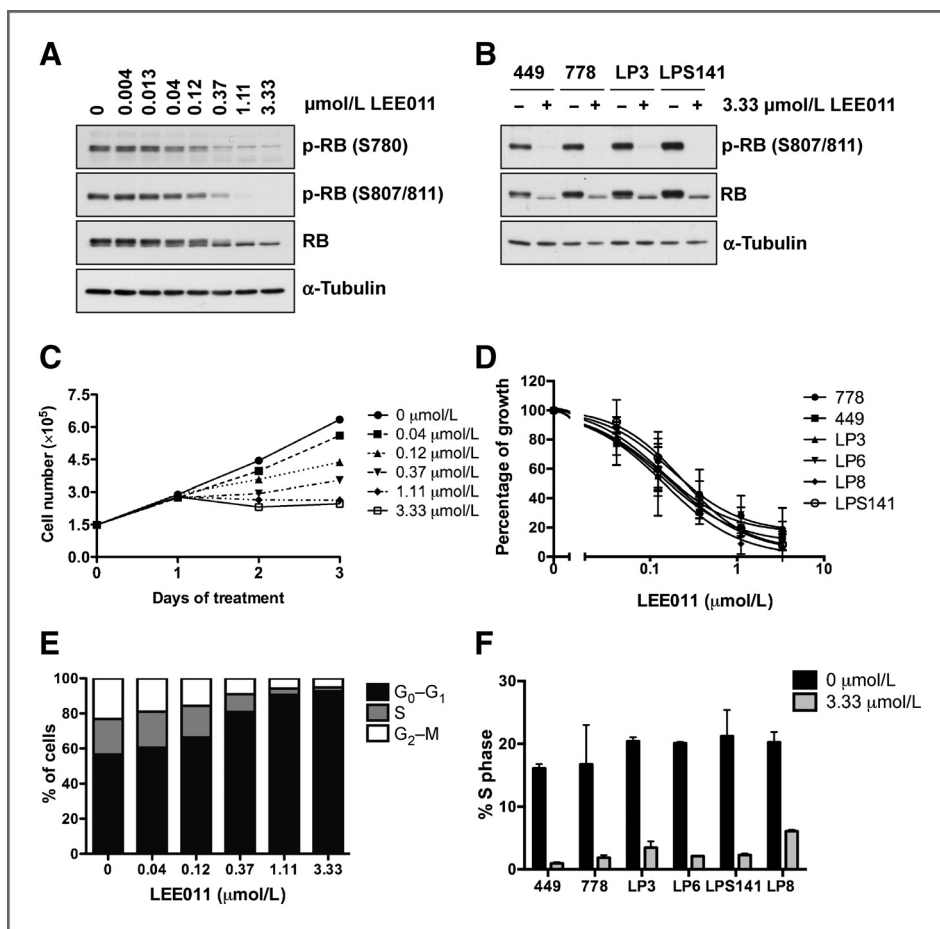
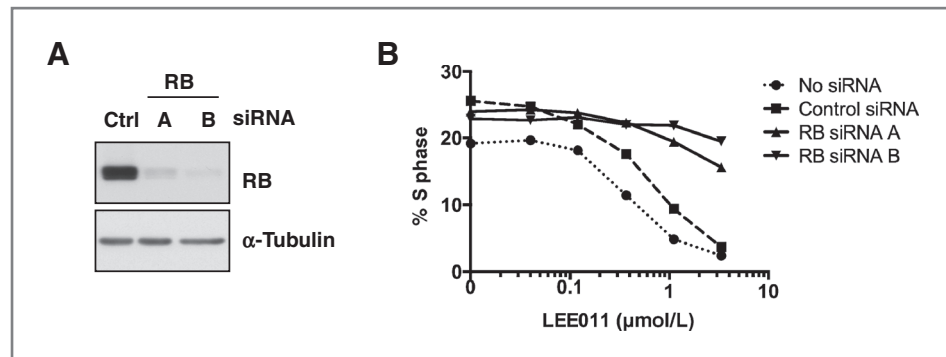


**Figure 3.** Effects of CDK4/6 inhibitor LEE011 on RB phosphorylation and cell growth in liposarcoma cells. **A** and **B**, effects of LEE011 on RB phosphorylation in LP6 (**A**) and other liposarcoma cells (**B**) were evaluated by immunoblot analysis at 24 hours. **C**, growth curves of LP6 cells treated with vehicle or LEE011 at indicated concentrations. Values represent mean  $\pm$  SEM ( $n = 2$ ). **D**, response of liposarcoma cells to 3 days treatment of LEE011. Values represent mean  $\pm$  SD ( $n = 2$ ). **E** and **F**, effects of LEE011 on cell-cycle distribution of liposarcoma cells at 24 hours. In **E**, LP6 cells were used; in **F**, values represent mean  $\pm$  SD ( $n = 2$ ).

**Figure 4.** siRNA-mediated knockdown of RB rescues the inhibitory effects of LEE011 in liposarcoma cells. **A**, siRNA-mediated knockdown of RB expression at 48 hours. **B**, LP6 cells were transfected with RB siRNA, control siRNA, or buffer only. LEE011 was added 48 hours after transfection and its effects on cell-cycle distribution were examined by flow-cytometric analysis at 24 hours. Data are representative of three independent experiments.



with two independent siRNA constructs to RB and then examined the effects of LEE011 on the RB-depleted liposarcoma cells. As shown in Fig. 4A and 4B, the observed induction of cell-cycle arrest by LEE011 was dramatically abrogated in LP6 cells transfected with RB siRNA, in comparison with cells transfected with control siRNA or without siRNA. Therefore, RB is a key mediator of LEE011-induced cell-cycle arrest and diminished cell growth in liposarcoma cells.

#### LEE011 reduces RB phosphorylation, BrdUrd incorporation, and tumor FDG uptake *in vivo*

To demonstrate the impact of LEE011 on tumor behavior *in vivo*, we employed a xenograft model of liposarcoma cell line LP6 and further investigated the effects of LEE011 treatment on RB phosphorylation and cell proliferation. As shown by immunoblot analysis and IHC staining, following treatment with three daily doses of LEE011 (250 mg/kg/d), RB phosphorylation at Ser780 was dramatically reduced and RB protein shifted to its hypophosphorylated form (Fig. 5A and B). In addition, *in vivo* BrdUrd incorporation into tumors was significantly decreased (Fig. 5B), indicative of reduced cell proliferation. We attempted to determine the *in vivo* effects on cellular proliferation using 3'-deoxy-3-[<sup>18</sup>F]-fluorothymidine (<sup>18</sup>F-FLT)-PET imaging, but there was no significant baseline FLT-PET signal in the liposarcoma xenograft models examined (data not shown).

To assess the impact of LEE011 treatment on tumor metabolism, we evaluated the *in vivo* <sup>18</sup>F-FDG-PET response to LEE011 in mice bearing the LP6 liposarcoma tumor xenograft model. Baseline <sup>18</sup>F-FDG-PET scans consistently identified aberrantly high tumor glucose utilization in the LP6 models (SUV<sub>max</sub>: ~2.0 or higher). After 3 days of treatment, the SUV<sub>max</sub> in the LP6 tumors of those mice treated with LEE011 dropped significantly by approximately 50%. In contrast, the tumor SUV<sub>max</sub> in vehicle-treated mice was either unchanged or slightly increased (Fig. 5C and D). These results suggest that LEE011 substantially alters tumor metabolism in the liposarcoma xenograft model.

#### LEE011 inhibits tumor growth *in vivo*

To determine whether the observed biologic effects of LEE011 treatment could be translated into clinically rel-

evant antitumor activity, liposarcoma growth was studied in established LP6 cell line xenografts as well as in LPS3 and HSAX2655 primary human liposarcoma tumor xenografts following LEE011 treatment. As shown in Fig. 5E and F, LEE011 significantly decreased growth of both LP6 (250 mg/kg/d, 21 days, orally) and LPS3 xenografts (250 mg/kg, 5 days on/2 days off for 3 weeks, orally) during the treatment ( $P < 0.001$  for LP6 xenografts,  $P < 0.05$  for LPS3 xenografts). No significant weight loss of the mice was observed in the mice treated with LEE011 (Supplementary Fig. S3A and S3B). The aggressively growing LP6 cell line xenograft eventually grew despite continued treatment with LEE011, albeit at a significantly slower rate than in mice treated with vehicle control (Fig. 5E). In contrast, the LPS3 primary liposarcoma xenograft continued to respond over the treatment period. Daily oral treatment with LEE011 (250 mg/kg) resulted in dramatic and durable tumor regression of the HSAX2655 primary liposarcoma xenografts, reaching 90% after 80 days of continuous treatment (Fig. 5G). No significant weight loss of the mice was observed in the HSAX2655-carrying mice treated with LEE011 (Supplementary Fig. S3C). We continued to monitor animals for tumor regrowth after suspension of drug treatment. Two out of 12 mice did not have palpable tumors at study termination on day 206 (91 days posttreatment cessation) and were considered complete regression. Tumors regrew in the remaining animals with varying sensitivity to retreatment with LEE011 (data not shown).

#### Cell-cycle re-entry following continuous chronic CDK4/6 inhibition *in vitro*

To further determine the possible causes of LP6 cell line xenograft tumor growth in the setting of prolonged LEE011 administration in contrast with the effects seen with short-term dosing, we examined the phosphorylation status of RB and the cell-cycle dynamics. Chronic continuous exposure to LEE011 led to gradual recovery of RB hyperphosphorylation at the CDK4/6-specific sites S780 and S807/811 and release from cell-cycle arrest after 4, 7, or 17 days (Fig. 6A). Concomitant with these changes, increases in cyclins D1, D2, and D3 expression were observed (Fig. 6B), which may reflect a compensatory feedback mechanism driving cell-cycle progression. The appearance of RB hyperphosphorylation and escape from

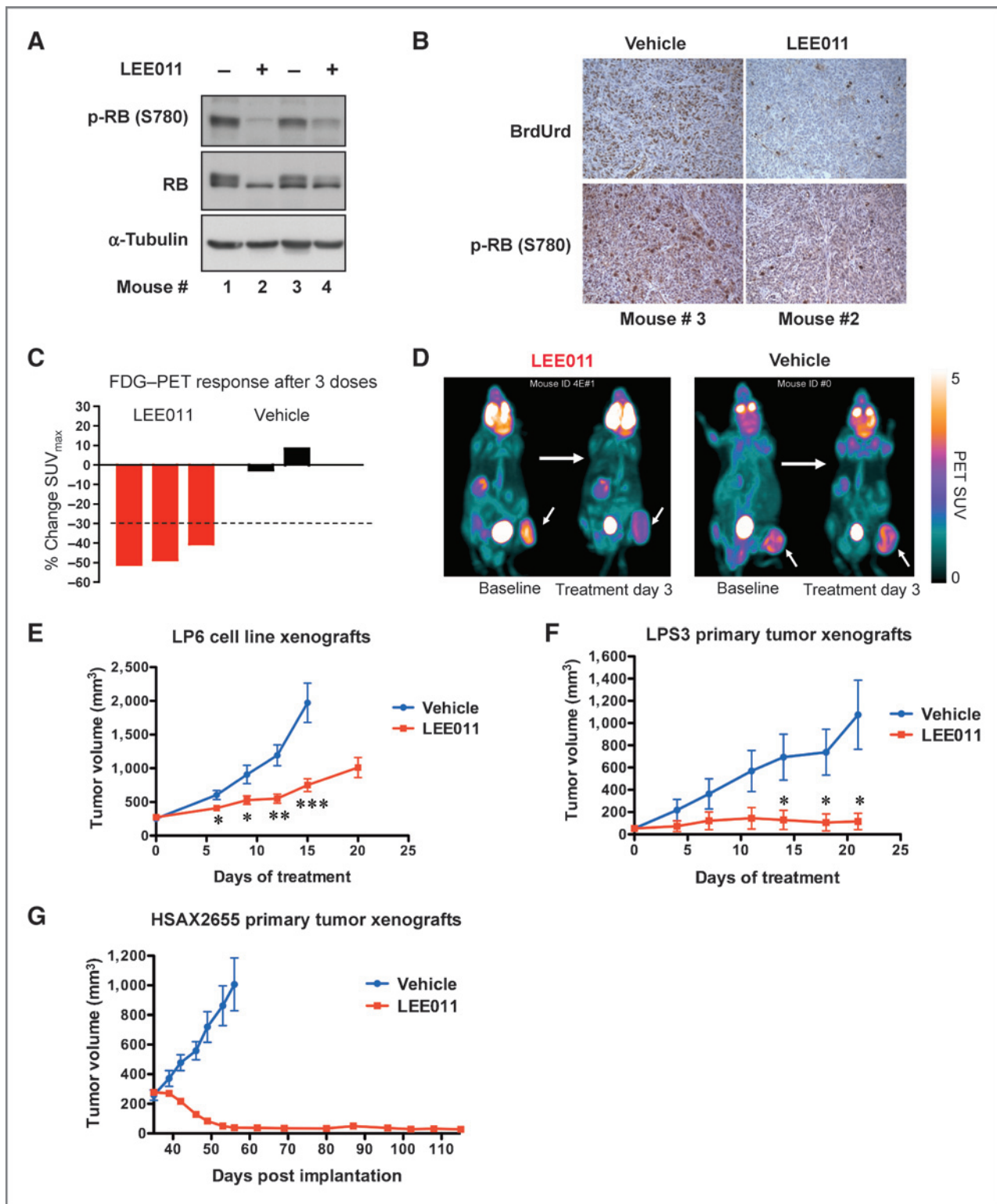
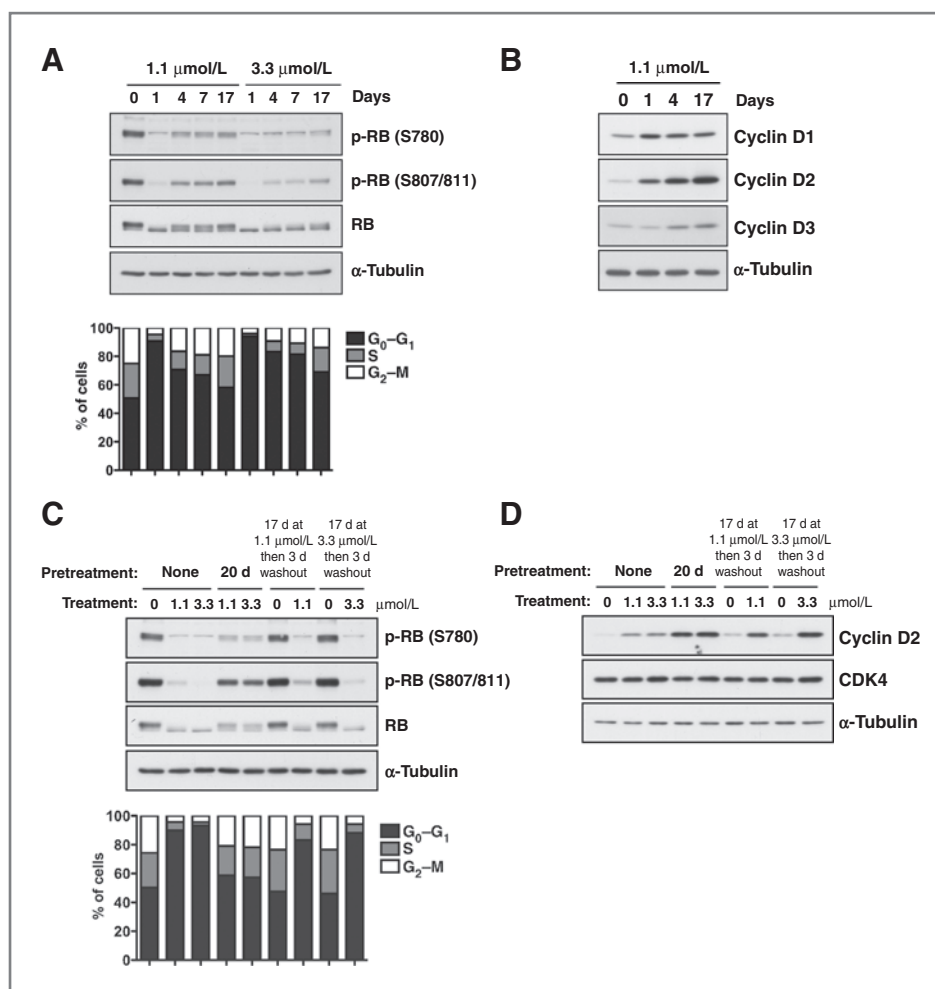


Figure 5. Effects of LEE011 treatment on RB phosphorylation, BrdUrd incorporation, tumor FDG uptake, and tumor growth *in vivo*. A and B, after three doses of LEE011 (250 mg/kg/d) or vehicle control, tumor samples were analyzed for *in vivo* BrdUrd incorporation. A, protein expression and phosphorylation in frozen LP6 tumor specimens were evaluated by immunoblot analyses. B, representative examples of IHC staining for BrdUrd and phospho-RB (Ser780) in LP6 tumor xenografts. Original magnification,  $\times 200$ . C and D, FDG-PET response after three doses of LEE011 (250 mg/kg/d) or vehicle control. C, change in  $^{18}\text{F}$ -FDG SUV<sub>max</sub> of LP6 tumors. Each bar represents a tumor lesion. D, representative PET imaging of LP6 xenografts. Small arrows, the anatomical location of tumor xenograft. Other areas of  $^{18}\text{F}$ -FDG signal represent the brain, heart, and bladder. (Continued on the following page.)

**Figure 6.** Continuous exposure to LEE011 leads to enhanced RB phosphorylation and reversible cell-cycle re-entry. A and B, LP6 cells were continuously exposed to LEE011 for the indicated time and concentrations. RB phosphorylation (A, top) and the expression of cyclin D (B) were examined by immunoblot analyses 24 hours after the last dose, and cell-cycle distribution was determined by flow cytometry analysis (A, bottom). C and D, LP6 cells with or without pretreatment were exposed to LEE011 for 24 hours. RB phosphorylation (C, top) and the expression of cyclin D2 and CDK4 (D) were examined by immunoblot analyses. Cell-cycle distribution was determined by flow-cytometric analysis (C, bottom).



cell-cycle arrest were completely reversible: following a 3-day washout period from LEE011, repeat exposure to drug again resulted in suppression of RB phosphorylation, and induction of  $G_0$ - $G_1$  arrest (Fig. 6C). Cyclin D2 expression similarly reverted to normal levels following drug washout but was reinduced in the presence of LEE011 (Fig. 6D). These data suggest a dynamic mechanism that may be induced with chronic exposure and which permits escape from cell-cycle arrest independent from presumed genetic selection of treatment-resistant subclones.

## Discussion

In this report, we define the critical role of CDK4 overexpression and activity in regulating liposarcoma

growth *in vitro* and *in vivo*. By using siRNA or a small-molecule inhibitor of CDK4/6, we observed RB hypophosphorylation, cell-cycle arrest, decreased DNA synthesis, decreased tumor glucose metabolism, and model-dependent tumor growth arrest or regression. The *CDK4* gene is significantly amplified in the vast majority of WD/DDLPS. Our findings validate the critical role of CDK4 in maintaining liposarcoma proliferation (18), metabolism, and survival, supporting the rationale for clinical development of CDK4 inhibitors for the treatment of WD/DDLPS. The inhibitory effects of LEE011 on cell-cycle progression required RB; therefore, the status of RB may be useful as a selective or predictive biomarker for clinical studies of CDK4/6 inhibitors.

(Continued.) E, established LP6 tumors were treated with 250 mg/kg LEE011 or with vehicle alone daily for 21 days by oral gavage. Tumor size was measured by caliper every 3 to 6 days. Mice were sacrificed when the tumor diameter reached 2 cm. Values represent mean volume  $\pm$  SEM ( $n \geq 8$ ); \*,  $P < 0.05$ ; \*\*,  $P < 0.01$ ; \*\*\*,  $P < 0.001$ ; compared with respective control group treated with vehicle. F, primary human liposarcoma xenograft LPS3 was treated with 250 mg/kg LEE011 or with vehicle alone by oral gavage following a 5 days on/2 days off schedule for 3 weeks. Tumor size was measured by caliper every 3 to 4 days. Values represent mean volume  $\pm$  SEM ( $n = 6$ ); \*,  $P < 0.05$ ; compared with respective control group treated with vehicle. G, primary human liposarcoma xenograft HSAX2655 was treated with 250 mg/kg LEE011 or with vehicle alone daily by oral gavage beginning 35 days after implantation and continued for 80 days. Tumor size was measured by caliper twice weekly. Values represent mean volume  $\pm$  SEM ( $n = 4$  in control group,  $n = 12$  in LEE011 group).



Distinct from the cell-cycle inhibitory effects seen *in vitro*, LEE011 induced tumor regression in one primary patient tumor xenograft model. This may reflect a greater dependency on CDK4/6 signaling in the context of the tumor/stromal environment, distinct from cell lines selected for their growth on plastic. Alternatively, this finding may indicate that in some tumor models, the endogenous apoptosis rate may become revealed by way of tumor regression once cell proliferation is abrogated and the cell growth/death balance is altered. A similar observation has been reported in studies with PD0332991 in other cancer types (28), wherein no cell death was observed *in vitro*, whereas *in vivo* treatment resulted in complete regressions in some tumor models. In addition, a CDK4/6 inhibitor caused apoptosis in Notch1-driven T-cell acute lymphoblastic leukemia (29), suggesting that synthetic lethal interactions between CDK4/6 inhibition and other pathways may drive cell death.

Based both on the proposed mechanism of action as well as our observations reported herein, the clinical consequences of CDK4 inhibition by LEE011 treatment may range from cell-cycle arrest to tumor regression. This should be factored into translationally focused clinical studies to determine the activity of CDK4 inhibitors in liposarcoma: the clinical trials should be designed primarily to detect changes in tumor growth rates rather than to solely measure radiographic shrinkage of tumor (conventional rates of anatomic tumor "response"). Indeed, a recent clinical study of the CDK4/6 inhibitor PD0332991 in patients with liposarcoma demonstrated a median progression-free survival of 18 weeks, with a radiographic response rate of only 3.4% (21). The significance of disease control rates in uncontrolled, single arm phase II studies is difficult to assess; however, and appropriate comparisons with the prestudy tumor growth rate or to control treatment arms should be included (30).

In addition, our findings suggest that chronic treatment with a CDK4/6 inhibitor can lead to gradual recovery of RB hyperphosphorylation at the CDK4/6-specific sites S780 and S807/811 and re-entry into the cell cycle in one liposarcoma model. The breakthrough of cell-cycle arrest does not appear to be due to selection of subclones of LP6 cells that are resistant to LEE011 on the basis of genetic alterations. Instead, removal of LEE011 led to rapid reestablishment of sensitivity to drug, suggesting a dynamic feedback mechanism that may support some level of cell cycle re-entry in this model, although the durable tumor control seen in the LPS3 and HSAX2655 xenografts indicates that this may not be a universal effect. The phase II study of PD0332991 in liposarcoma used a 14-day on/7-day off dosing schedule, selected on the basis of determination of the maximum tolerated dose in a phase I study (31). Our observations suggest that this intermittent schedule may have been a fortuitous study design that enhanced antitumor activity by avoiding this potential feedback mechanism, although further exploration of dosing schedules with correlative pharmacodynamic studies will be essential to maximize

RB hypophosphorylation, cell-cycle arrest, and antitumor activity.

Compensatory upregulation of cyclin D1, D2, and D3 expression was also observed following LEE011 treatment. The precise mechanism of cyclin D induction and its biochemical consequences remain to be determined, although this was not the trivial result of accumulation of cells at the G<sub>1</sub>-S boundary, because flow-cytometric analysis showed a decreased proportion of cells at this point in the cell cycle as they again reestablished a normal cell-cycle profile. Deregulated expression of cyclin D has been shown to promote mitogen-independent proliferation as well as other cellular processes (9, 32). Whether the elevated level of cyclin D following LEE011 treatment contributed to the recovery of RB hyperphosphorylation and reentry into the cell cycle requires further investigation.

WD/DDLPs characteristically also have amplification of the *MDM2* gene (12), the product of which inhibits the activity of the p53 tumor suppressor and targets it for proteasomal degradation (33–35). By reactivating p53, small-molecule inhibitors of the MDM2-p53 interaction induce cell-cycle arrest and apoptosis (36). Inhibitors of this sort are currently in clinical development, and a recent study showed limited activity in patients with liposarcoma (37). Whether combined inhibition of CDK4 and MDM2 would lead to greater antitumor activity remains an area of active exploration.

In summary, our study reveals the important CDK4-RB signaling axis that directly regulates cell cycle and cell proliferation for the growth of liposarcoma *in vitro* and *in vivo*. Treatment with a CDK4/6 inhibitor is effective, but the waning response with continuous exposure suggests a reversible feedback mechanism that should be further explored and taken into account in the design of rationally designed translational clinical trials employing small-molecule CDK4/6 inhibitors.

#### Disclosure of Potential Conflicts of Interest

G.D. Demetri received a commercial research grant from Novartis and Pfizer, has ownership interest (including patents) in G1 Therapeutics, and is a consultant/advisory board member for Novartis, Pfizer, and G1 Therapeutics. A.J. Wagner is a consultant/advisory board member for Novartis. No potential conflicts of interest were disclosed by the other authors.

#### Authors' Contributions

**Conception and design:** Y.-X. Zhang, C. Brain, G.D. Demetri, S. Kim, A.J. Wagner

**Development of methodology:** Y.-X. Zhang, Y. Wang, A. Loo, A.J. Wagner  
**Acquisition of data (provided animals, acquired and managed patients, provided facilities, etc.):** Y.-X. Zhang, E. Sicinska, J.T. Czaplinski, S.P. Remillard, S. Moss, Y. Wang, A. Loo, A.L. Kung, A.J. Wagner

**Analysis and interpretation of data (e.g., statistical analysis, biostatistics, computational analysis):** Y.-X. Zhang, E. Sicinska, S.P. Remillard, Y. Wang, A. Loo, G.D. Demetri, S. Kim, A.L. Kung, A.J. Wagner  
**Writing, review, and/or revision of the manuscript:** Y.-X. Zhang, J.T. Czaplinski, S.P. Remillard, A. Loo, E.L. Snyder, G.D. Demetri, S. Kim, A.J. Wagner

**Administrative, technical, or material support (i.e., reporting or organizing data, constructing databases):** Y.-X. Zhang, J.T. Czaplinski, G.D. Demetri, A.J. Wagner

**Study supervision:** A. Loo, G.D. Demetri, A.J. Wagner

**Other (provided cell lines):** E.L. Snyder

## Acknowledgments

The authors thank Dr. Wolfram Goessling for critical review of the article.

## Grant Support

This work was supported by Virginia and D.K. Ludwig Fund for Cancer Research (to G.D. Demetri), the Peter and Paula Fasseas Fund for Lipo-

sarcoma Research (to A.J. Wagner), and the Liposarcoma Research Fund (to A.J. Wagner).

Received May 5, 2014; revised June 25, 2014; accepted July 8, 2014; published OnlineFirst July 15, 2014.

## References

- Classon M, Harlow E. The retinoblastoma tumour suppressor in development and cancer. *Nat Rev Cancer* 2002;2:910–7.
- Knudsen ES, Knudsen KE. Tailoring to RB: tumour suppressor status and therapeutic response. *Nat Rev Cancer* 2008;8:714–24.
- Harbour JW, Luo RX, Dei Santi A, Postigo AA, Dean DC. Cdk phosphorylation triggers sequential intramolecular interactions that progressively block Rb functions as cells move through G1. *Cell* 1999;98:859–69.
- Malumbres M, Barbacid M. To cycle or not to cycle: a critical decision in cancer. *Nat Rev Cancer* 2001;1:222–31.
- Zarkowska T, Mittnacht S. Differential phosphorylation of the retinoblastoma protein by G1/S cyclin-dependent kinases. *J Biol Chem* 1997;272:12738–46.
- Bockstaele L, Kooken H, Libert F, Paternot S, Dumont JE, de Launoit Y, et al. Regulated activating Thr172 phosphorylation of cyclin-dependent kinase 4(CDK4): its relationship with cyclins and CDK "inhibitors". *Mol Cell Biol* 2006;26:5070–85.
- Bockstaele L, Coulonval K, Kooken H, Paternot S, Roger PP. Regulation of CDK4. *Cell Div* 2006;1:25.
- Kim JK, Diehl JA. Nuclear cyclin D1: an oncogenic driver in human cancer. *J Cell Physiol* 2009;220:292–6.
- Musgrove EA, Caldon CE, Barraclough J, Stone A, Sutherland RL. Cyclin D as a therapeutic target in cancer. *Nat Rev Cancer* 2011;11:558–72.
- Roussel MF. The INK4 family of cell cycle inhibitors in cancer. *Oncogene* 1999;18:5311–7.
- Ortega S, Malumbres M, Barbacid M. Cyclin D-dependent kinases, INK4 inhibitors and cancer. *Biochim Biophys Acta* 2002;1602:73–87.
- Sirvent N, Coindre JM, Maire G, Hostein I, Keslair F, Guillou L, et al. Detection of MDM2-CDK4 amplification by fluorescence *in situ* hybridization in 200 paraffin-embedded tumor samples: utility in diagnosing adipocytic lesions and comparison with immunohistochemistry and real-time PCR. *Am J Surg Pathol* 2007;31:1476–89.
- Binh MB, Sastre-Garau X, Guillou L, de Pinieux G, Terrier P, Lagace R, et al. MDM2 and CDK4 immunostainings are useful adjuncts in diagnosing well-differentiated and dedifferentiated liposarcoma subtypes: a comparative analysis of 559 soft tissue neoplasms with genetic data. *Am J Surg Pathol* 2005;29:1340–7.
- Henze J, Bauer S. Liposarcomas. *Hematol Oncol Clin North Am* 2013;27:939–55.
- Conyers R, Young S, Thomas DM. Liposarcoma: molecular genetics and therapeutics. *Sarcoma* 2011;2011:483154.
- Crago AM, Singer S. Clinical and molecular approaches to well differentiated and dedifferentiated liposarcoma. *Curr Opin Oncol* 2011;23:373–8.
- Ghadimi MP, Al-Zaid T, Madewell J, Peng T, Colombo C, Hoffman A, et al. Diagnosis, management, and outcome of patients with dedifferentiated liposarcoma systemic metastasis. *Ann Surg Oncol* 2011;18:3762–70.
- Heliass-Rodzewicz Z, Pedeutour F, Coindre JM, Terrier P, Aurias A. Selective elimination of amplified CDK4 sequences correlates with spontaneous adipocytic differentiation in liposarcoma. *Genes Chromosomes Cancer* 2009;48:943–52.
- Barretina J, Taylor BS, Banerji S, Ramos AH, Lagos-Quintana M, Decarolis PL, et al. Subtype-specific genomic alterations define new targets for soft-tissue sarcoma therapy. *Nat Genet* 2010;42:715–21.
- Miller ML, Molinelli EJ, Nair JS, Sheikh T, Samy R, Jing X, et al. Drug synergy screen and network modeling in dedifferentiated liposarcoma identifies CDK4 and IGF1R as synergistic drug targets. *Sci Signal* 2013;6:ra85.
- Dickson MA, Tap WD, Keohan ML, D'Angelo SP, Gounder MM, Antonescu CR, et al. Phase II trial of the CDK4 inhibitor PD0332991 in patients with advanced CDK4-amplified well-differentiated or dedifferentiated liposarcoma. *J Clin Oncol* 2013;31:2024–8.
- Pedeutour F, Forus A, Coindre JM, Berner JM, Nicolo G, Michiels JF, et al. Structure of the supernumerary ring and giant rod chromosomes in adipose tissue tumors. *Genes Chromosomes Cancer* 1999;24:30–41.
- Snyder EL, Sandstrom DJ, Law K, Fiore C, Sicinska E, Brito J, et al. c-Jun amplification and overexpression are oncogenic in liposarcoma but not always sufficient to inhibit the adipocytic differentiation programme. *J Pathol* 2009;218:292–300.
- Peng XD, Xu PZ, Chen ML, Hahn-Windgassen A, Skeen J, Jacobs J, et al. Dwarfism, impaired skin development, skeletal muscle atrophy, delayed bone development, and impeded adipogenesis in mice lacking Akt1 and Akt2. *Genes Dev* 2003;17:1352–65.
- Kim S, Loo A, Chopra R, Caponigro G, Huang A, Vora S, et al. LEE011: an orally bioavailable, selective small molecule inhibitor of CDK4/6-reactivating Rb in cancer. *Mol Cancer Ther* 2013;12:11s. (suppl; abstr PR02).
- Chen Z, Cheng K, Walton Z, Wang Y, Ebi H, Shimamura T, et al. A murine lung cancer co-clinical trial identifies genetic modifiers of therapeutic response. *Nature* 2012;483:613–7.
- Infante JR, Shapiro GI, Witteveen PO, geracitano JF, Ribrag V, chugh R, et al. Phase I multicenter, open label, dose-escalation study of LEE011, an oral inhibitor of cyclin-dependent kinase 4/6, in patients with advanced solid tumors or lymphomas. *Mol Cancer Ther* 2013;12:11s. (suppl; abstr A276).
- Fry DW, Harvey PJ, Keller PR, Elliott WL, Meade M, Trachet E, et al. Specific inhibition of cyclin-dependent kinase 4/6 by PD 0332991 and associated antitumor activity in human tumor xenografts. *Mol Cancer Ther* 2004;3:1427–38.
- Choi YJ, Li X, Hydrbring P, Sanda T, Stefano J, Christie AL, et al. The requirement for cyclin D function in tumor maintenance. *Cancer Cell* 2012;22:438–51.
- Sleijfer S, Wagner AJ. The challenge of choosing appropriate end points in single-arm phase II studies of rare diseases. *J Clin Oncol* 2012;30:896–8.
- Schwartz GK, LoRusso PM, Dickson MA, Randolph SS, Shaik MN, Wilner KD, et al. Phase I study of PD 0332991, a cyclin-dependent kinase inhibitor, administered in 3-week cycles (schedule 2/1). *Br J Cancer* 2011;104:1862–8.
- Wang TC, Cardiff RD, Zukerberg L, Lees E, Arnold A, Schmidt EV. Mammary hyperplasia and carcinoma in MMTV-cyclin D1 transgenic mice. *Nature* 1994;369:669–71.
- Momand J, Zambetti GP, Olson DC, George D, Levine AJ. The mdm-2 oncogene product forms a complex with the p53 protein and inhibits p53-mediated transactivation. *Cell* 1992;69:1237–45.
- Haupt Y, Maya R, Kazaz A, Oren M. Mdm2 promotes the rapid degradation of p53. *Nature* 1997;387:296–9.
- Kubbutat MH, Jones SN, Vousden KH. Regulation of p53 stability by Mdm2. *Nature* 1997;387:299–303.
- Muller CR, Paulsen EB, Noordhuis P, Pedeutour F, Saeter G, Myklebost O. Potential for treatment of liposarcomas with the MDM2 antagonist Nutlin-3A. *Int J Cancer* 2007;121:199–205.
- Ray-Coquard I, Blay JY, Italiano A, Le Cesne A, Penel N, Zhi J, et al. Effect of the MDM2 antagonist RG7112 on the P53 pathway in patients with MDM2-amplified, well-differentiated or dedifferentiated liposarcoma: an exploratory proof-of-mechanism study. *Lancet Oncol* 2012;13:1133–40.